

Pure Spin Current Injection in Hydrogenated Graphene Structures

Reinaldo Zapata-Peña¹, Bernardo S. Mendoza¹, Anatoli I. Shkrebtii²

¹*Centro de Investigaciones en Óptica, León, Guanajuato 37150, México and*

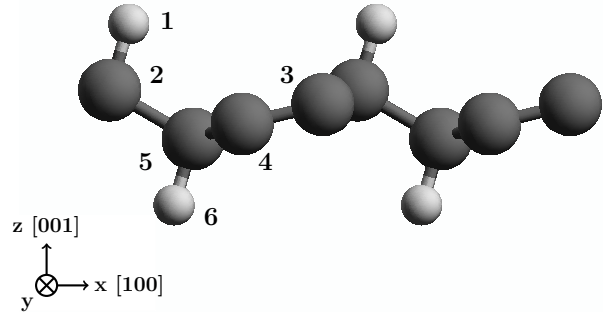
²*University of Ontario, Institute of Technology, Oshawa, ON, L1H 7L7, Canada*

(Dated: April 24, 2017)

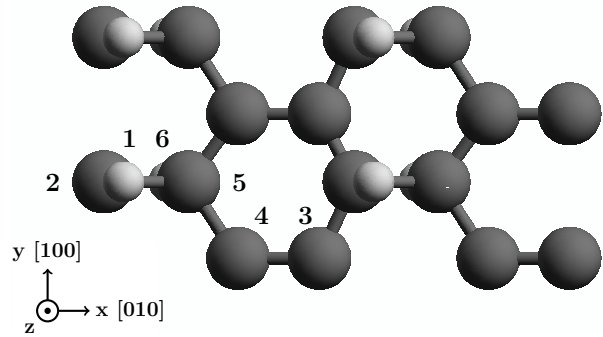
Lorem ipsum dolor sit amet, consectetur adipiscing elit. Etiam lobortis facilisis sem. Nullam nec mi et neque pharetra sollicitudin. Praesent imperdiet mi nec ante. Donec ullamcorper, felis non sodales commodo, lectus velit ultrices augue, a dignissim nibh lectus placerat pede. Vivamus nunc nunc, molestie ut, ultricies vel, semper in, velit. Ut porttitor. Praesent in sapien. Lorem ipsum dolor sit amet, consectetur adipiscing elit. Duis fringilla tristique neque. Sed interdum libero ut metus. Pellentesque placerat. Nam rutrum augue a leo. Morbi sed elit sit amet ante lobortis sollicitudin. Praesent blandit blandit mauris. Praesent lectus tellus, aliquet aliquam, luctus a, egestas a, turpis. Mauris lacinia lorem sit amet ipsum. Nunc quis urna dictum turpis accumsan semper.

I. INTRODUCTION

Lorem ipsum dolor sit amet, consectetur adipiscing elit. Etiam lobortis facilisis sem. Nullam nec mi et neque pharetra sollicitudin. Praesent imperdiet mi nec ante. Donec ullamcorper, felis non sodales commodo, lectus velit ultrices augue, a dignissim nibh lectus placerat pede. Vivamus nunc nunc, molestie ut, ultricies vel, semper in, velit. Ut porttitor. Praesent in sapien. Lorem ipsum dolor sit amet, consectetur adipiscing elit. Duis fringilla tristique neque. Sed interdum libero ut metus. Pellentesque placerat. Nam rutrum augue a leo. Morbi sed elit sit amet ante lobortis sollicitudin. Praesent blandit blandit mauris. Praesent lectus tellus, aliquet aliquam, luctus a, egestas a, turpis. Mauris lacinia lorem sit amet ipsum. Nunc quis urna dictum turpis accumsan semper. Lorem ipsum dolor sit amet, consectetur adipiscing elit. Etiam lobortis facilisis sem. Nullam nec mi et neque pharetra sollicitudin. Praesent imperdiet mi nec ante. Donec ullamcorper, felis non sodales commodo, lectus velit ultrices augue, a dignissim nibh lectus placerat pede. Vivamus nunc nunc, molestie ut, ultricies vel, semper in, velit. Ut porttitor. Praesent in sapien. Lorem ipsum dolor sit amet, consectetur adipiscing elit. Duis fringilla tristique neque. Sed interdum libero ut metus. Pellentesque placerat. Nam rutrum augue a leo. Morbi sed elit sit amet ante lobortis sollicitudin. Praesent blandit blandit mauris. Praesent lectus tellus, aliquet aliquam, luctus a, egestas a, turpis. Mauris lacinia lorem sit amet ipsum. Nunc quis urna dictum turpis accumsan semper.



(a) xz plane view



(b) xy plane view

FIG. 1. Alt structure.

tus tellus, aliquet aliquam, luctus a, egestas a, turpis. Mauris lacinia lorem sit amet ipsum. Nunc quis urna dictum turpis accumsan semper.

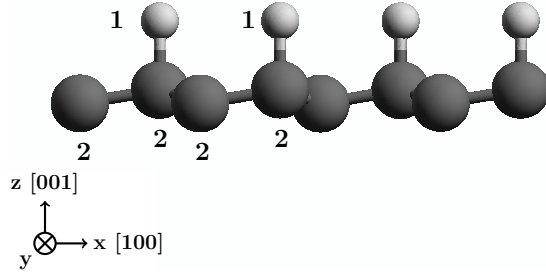
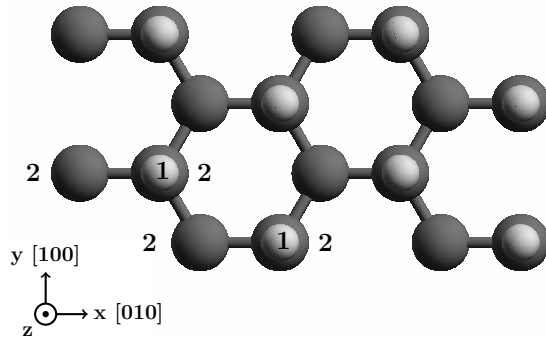
(a) xz plane view(b) xy plane view

FIG. 2. Up structure

Lorem ipsum dolor sit amet, consectetur adipiscing elit. Etiam lobortis facilisis sem. Nullam nec mi et neque pharetra sollicitudin. Praesent imperdiet mi nec ante. Donec ullamcorper, felis non sodales commodo, lectus velit ultrices augue, a dignissim nibh lectus placerat pede. Vivamus nunc nunc, molestie ut, ultricies vel, semper in, velit. Ut porttitor. Praesent in sapien.

vamus nunc nunc, molestie ut, ultricies vel, semper in, velit. Ut porttitor. Praesent in sapien. Lorem ipsum dolor sit amet, consectetur adipiscing elit. Duis fringilla tristique neque. Sed interdum libero ut metus. Pellentesque placerat. Nam rutrum augue a leo. Morbi sed elit sit amet ante lobortis sollicitudin. Praesent blandit blandit mauris. Praesent lectus tellus, aliquet aliquam, luctus a, egestas a, turpis. Mauris lacinia lorem sit amet ipsum. Nunc quis urna dictum turpis accumsan semper.

Lorem ipsum dolor sit amet, consectetur adipiscing elit. Etiam lobortis facilisis sem. Nullam nec mi et neque pharetra sollicitudin. Praesent imperdiet mi nec ante. Donec ullamcorper, felis non sodales commodo, lectus velit ultrices augue, a dignissim nibh lectus placerat pede. Vivamus nunc nunc, molestie ut, ultricies vel, semper in, velit. Ut porttitor. Praesent in sapien. Lorem ipsum dolor sit amet, consectetur adipiscing elit. Duis fringilla tristique neque. Sed interdum libero ut metus. Pellentesque placerat. Nam rutrum augue a leo. Morbi sed elit sit amet ante lobortis sollicitudin. Praesent blandit blandit mauris. Praesent lectus tellus, aliquet aliquam, luctus a, egestas a, turpis. Mauris lacinia lorem sit amet ipsum. Nunc quis urna dictum turpis accumsan semper.

II. THEORY

The equation for \mathcal{V}^{ab} for normal incidence in the xy plane with a polarization angle α is given by

$$\begin{aligned} \mathcal{V}^{ab}(\omega) &= \frac{2\mu^{abxx}(\omega)E^2(\omega)\cos^2(\alpha) + \mu^{abyy}(\omega)E^2(\omega)\sin^2(\alpha) + 2\mu^{abxy}(\omega)E^2(\omega)\cos(\alpha)\sin(\alpha)}{\xi^{xx}(\omega)E^2(\omega)\cos^2(\alpha) + \xi^{yy}(\omega)E^2(\omega)\sin^2(\alpha)}, \\ &= \frac{2\mu^{abxx}(\omega)\cos^2(\alpha) + \mu^{abyy}(\omega)\sin^2(\alpha) + \mu^{abxy}(\omega)\sin(2\alpha)}{\xi^{xx}(\omega)\cos^2(\alpha) + \xi^{yy}(\omega)\sin^2(\alpha)}. \end{aligned} \quad (1)$$

For an angle $\alpha = \frac{\pi}{4}$ this expression can be reduced to

$$\mathcal{V}^{ab}(\omega) = \frac{2\mu^{abxx}(\omega) + \mu^{abyy}(\omega) + 2\mu^{abxy}(\omega)}{\xi^{xx}(\omega) + \xi^{yy}(\omega)}. \quad (2)$$

A. Fixing velocity.

Considering that we have 2D structures we fixed the velocity in the xy plane along x and y directions and we define $|\mathcal{V}^a|$ as

$$|\mathcal{V}^a| = \sqrt{(\mathcal{V}^{ax})^2 + (\mathcal{V}^{ay})^2 + (\mathcal{V}^{az})^2}, \quad (3)$$

and the corresponding polar and azimuthal angles θ and φ as

$$\theta = \cos^{-1} \left(\frac{\mathcal{V}^{az}}{|\mathcal{V}^a|} \right), \quad 0 \leq \theta \leq \pi, \quad (4)$$

$$\varphi = \tan^{-1} \left(\frac{\mathcal{V}^{ay}}{\mathcal{V}^{ax}} \right), \quad 0 \leq \varphi \leq 2\pi. \quad (5)$$

B. Fixing spin

In a similar way we can fix in the xy plane the spin direction along the x , y , and z directions and then define the magnitude of the spin velocity $|\mathcal{V}_{\sigma^b}|$ in a fixed angle γ_b

$$|\mathcal{V}_{\sigma^b}| = \sqrt{(\mathcal{V}^{ax})^2 + (\mathcal{V}^{ay})^2}, \quad (6)$$

$$\gamma_b = \tan^{-1} \left(\frac{\mathcal{V}^{ay}}{\mathcal{V}^{ax}} \right), \quad (7)$$

where the angle is measured in the counter-clockwise direction from the positive x axis.

III. RESULTS

We preset the results for \mathcal{V}^{ab} for the C_{16}H_8 -alt and C_{16}H_8 -up structures being both noncentrosymmetric semi-infinite carbon systems with 50% hydrogenation in different arrangements. The *alt* system has alternating hydrogen atoms on the upper and bottom sides of the carbon sheet, while the *up* system has H only on the upper side. We take the hexagonal carbon lattice to be on the xy plane for both structures, and the carbon-hydrogen bonds on the perpendicular xz plane, as depicted in Figs. 1 and 2.

Using the ABINIT code¹ we calculated the self-consistent ground state and the Kohn-Sham states using density functional theory in the local density approximation (DFT-LDA) with a planewave basis. We used Hartwigsen-Goedecker-Hutter (HGH) relativistic separable

Layer No.	Atom type	Position [\AA]		
		x	y	z
1	H	-0.61516	-1.42140	1.47237
2	C	-0.61516	-1.73300	0.39631
3	C	0.61516	1.73300	0.15807
4	C	0.61516	0.42201	-0.15814
5	C	-0.61516	-0.37396	-0.39632
6	H	-0.61516	-0.68566	-1.47237

TABLE I. Unit cell of *alt* structure. Layer division, atom types and positions for the *alt* structure. The structure unit cell was divided in six layers corresponding each one to atoms in different z positions. The corresponding layer atom position is depicted in Fig. 1 with the corresponding number of layer.

dual-space Gaussian pseudopotentials² including the spin-orbit interaction for calculating $\mathcal{V}^a(\omega)$.

The convergence parameters for the calculations of our results corresponding to the *alt* and *up* structures are cutoff energies of 65 Ha and 40 Ha, respectively. The energy eigenvalues and matrix elements were calculated using 14452 \mathbf{k} points and 8452 \mathbf{k} points in the irreducible Brillouin zone (IBZ) and present LDA energy band gaps of 0.72 eV and 0.088 eV, respectively for the *alt* and *up* structures. As mentioned in³, using DFT the LDA is only one method of many other that can be used to calculate the electronic structure of materials. Also it is known that all methods predict a different band gap than the obtained in the experiment. A correction for the band gap energy value can be calculated by other *ab-initio* methods such as the GW approximation⁴ being this outside the scope of this paper.

The structures presented here were divided into layers to analyze the layer-by-layer contribution for \mathcal{V}^{ab} response. The *alt* structure was divided in six layers corresponding the first one to the top hydrogen atoms, from the second to the forth to carbon atoms in different z positions, and the sixth and last one to the bottom hydrogen atoms. The *up* structure was divided into two layers, the first one comprised by the top hydrogen atoms and the second by the carbon atoms. The layer divisions and atom positions for the unit cells are shown in Tables I and II.

Layer No.	Atom type	Position [\AA]		
		x	y	z
1	H	-0.61516	-1.77416	0.73196
1	H	0.61518	0.35514	0.73175
2	C	-0.61516	-1.77264	-0.49138
2	C	-0.61516	-0.35600	-0.72316
2	C	0.61516	0.35763	-0.49087

TABLE II. Unit cell of *up* structure. Layer division, atom types and positions for the *up* structure. The structure unit cell was divided in two layers corresponding to hydrogen and carbon atoms. The corresponding layer atom position is depicted in Fig. 2 with the corresponding number of layer.

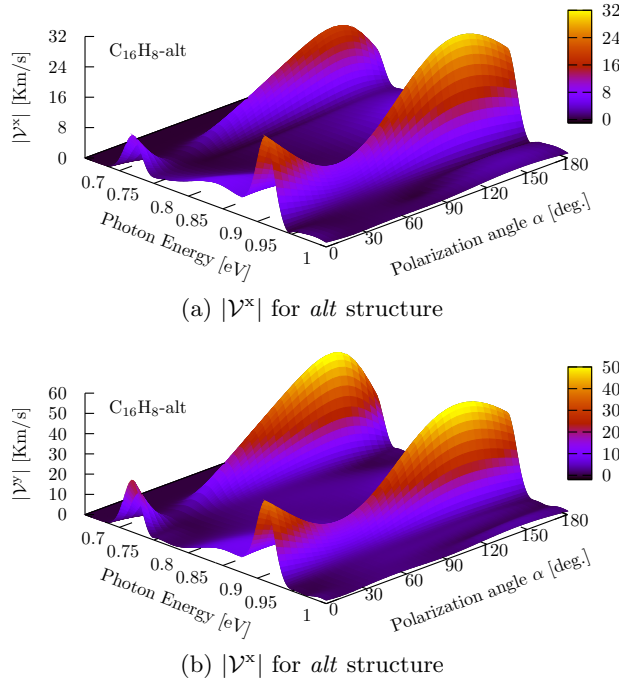


FIG. 3. $|V^x|$ response for $C_{16}H_8$ -alt structure. The maximum response zone is localized for an energy range from 0.90 eV to 0.93 eV, 145° and for a polarization angle of the incoming beam from 120° to 150° .

A. Fixing velocity

For the *alt* structure we analyzed the energy range of energy from 0.6 eV to 1.0 eV where we found the most intense response for V^{ab} and V^a . In Fig. 3 we present the $|V^a|$ spectra resulting from evaluate Eq. (3) using different polarization angles α in Eq. (1) for the $C_{16}H_8$ -alt

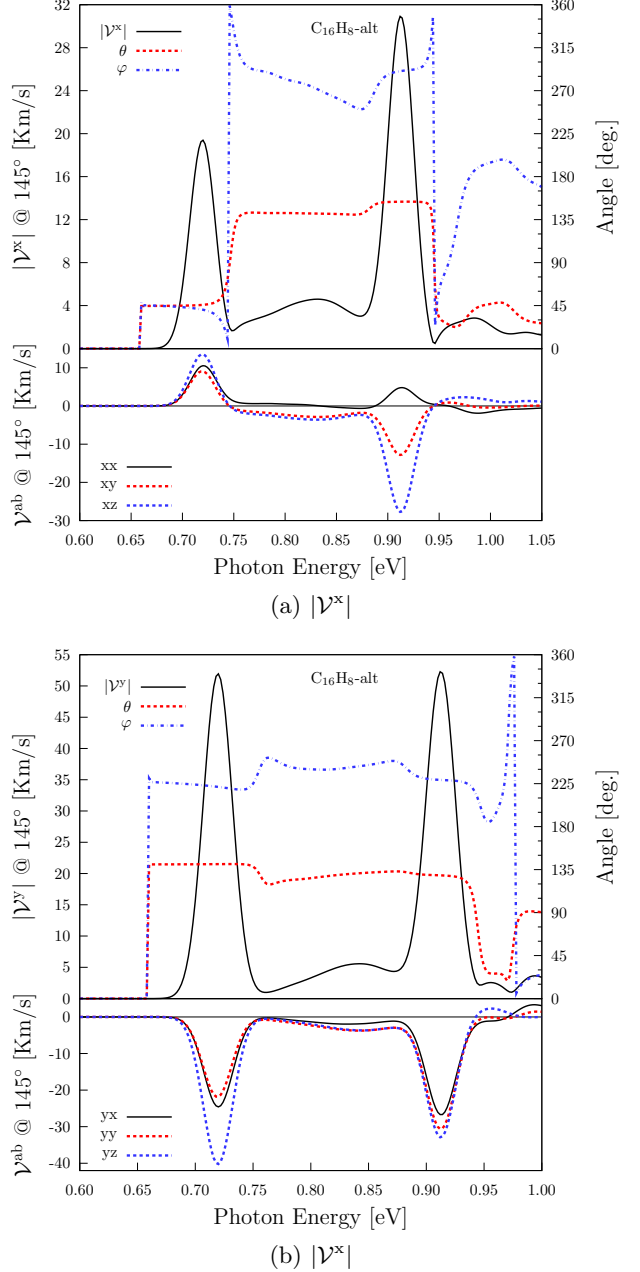


FIG. 4. Most intense responses of $|V^x|$ and $|V^y|$ and the corresponding three components for the *alt* structure. Both maxima were obtained for a polarization angle $\alpha = 145^\circ$.

structure. We can see that the onset of the response is when the energy of the incoming light is the same of the gap energy. From this picture we can see that for the zone between the energy range of 0.90 eV-0.93 eV and polarization angles between 120° and 150° is the zone of the absolute maximum response for both, $|V^x|$

and $|\mathcal{V}^y|$. Also there is another zone of interest for energies from 0.70 eV to 0.74 eV where a local maximum is obtained. From Fig. 3(a) we have that $|\mathcal{V}^x|$ reaches values near to 30 Km/s for the first zone mentioned before and 20 Km/s for the second one. We also found that the absolute maximum of the response is obtained when the polarization angle is $\alpha = 145^\circ$. In the top frames of Figs. 4(a) and 4(b) we present the results for $|\mathcal{V}^x|$ and $|\mathcal{V}^y|$ fixing the polarization angle to 145° for the *alt* structure vs the photon energy and the corresponding azimuthal θ and polar φ angles. Also in the bottom frames of Figs. 4(a) and 4(b) we present the decomposition of $|\mathcal{V}^x|$ and $|\mathcal{V}^y|$ in the corresponding \mathcal{V}^{xx} , \mathcal{V}^{xy} , \mathcal{V}^{xz} and \mathcal{V}^{yx} , \mathcal{V}^{yy} , \mathcal{V}^{yz} components for the fixed polarization angle. Making the analysis for the components and angles for $|\mathcal{V}^x|$ we can see that for the energy range from 0.70 eV to 0.74 eV all the *xx*, *xy*, and *xz* components contribute with almost the same intensity giving a total spin-velocity near to 30 Km/s and spin angles θ and φ near to 45.8° and 40.7° , respectively. In the other hand, for the energy range

from 0.88 eV to 0.95 eV there is a major contribution coming from the \mathcal{V}^{xz} component resulting in a spin-velocity magnitude near to 20 Km/s. In this case the spin angle over the *xy* plane have values near to 290° and the corresponding polar angle correspond to values near to 153° . Also we notice that for the range of 0.70-0.74 eV all the contributions are positive while for the range of 0.88-0.95 eV the *xx* component remains positive but the components *xy* and *xz* change in direction. This is due to **a change in the spin polarization**. Making now the analysis for $|\mathcal{V}^y|$, we notice that this response is almost two times more intense than $|\mathcal{V}^x|$. For the energy range from 0.70 eV to 0.74 eV the *yz* component have a more intense response than *yx* and *yy* components. This results in a spin azimuthal angle near to 221° and polar angle near to 141° . For the energy range all three components have almost the same intensity resulting in a spin-velocity near to 50 Km/s in both cases. Now we have that the three components of $|\mathcal{V}^y|$ are negative for the energy range from 0.65 eV to 0.95 eV **keeping the same spin polarization for all this range**.

¹ X. Gonze, B. Amadon, P.-M. Anglade, J.-M. Beuken, F. Bottin, P. Boulanger, F. Bruneval, D. Caliste, R. Caracas, M. Côté, T. Deutsch, L. Genovese, P. Ghosez, M. Giantomassi, S. Goedecker, D. Hamann, P. Hermet, F. Jollet, G. Jomard, S. Leroux, M. Mancini, S. Mazevet, M. Oliveira, G. Onida, Y. Pouillon, T. Rangel, G.-M. Rignanese, D. Sangalli, R. Shaltaf, M. Torrent, M. Verstraete, G. Zerah, and J. Zwanziger, Com-

put. Phys. Commun. **180**, 2582 (2009).

² C. Hartwigsen, S. Goedecker, and J. Hutter, Phys. Rev. B **58**, 3641 (1998).

³ R. Zapata-Peña, S. M. Anderson, B. S. Mendoza, and A. I. Shkrebtii, physica status solidi (b) **253**, 226 (2016).

⁴ G. Onida, L. Reining, and A. Rubio, Rev. Mod. Phys. **74**, 601 (2002).